# Multi-Messenger Detectability of Neutron Star Mergers and Gamma-Ray Bursts

Haoxiang LIN (林 浩翔)

The University of Tokyo
(Postdoc Fellow@KIAA since July 2022)

Supported by KAKENHI No.20J12200

Background: Beabudai Design

# Multi-messenger (MM) detection of binary neutron star (BNS) mergers

- What we already saw from GW170817
  - Gravitational waves, short GRB + afterglow, Kilonova
  - X-ray excess 3.5 yr later (Hajela+22, ApJL, 927, L17)
- Other potential messengers of interest
  - Very-high-energy gamma-rays (**this work**)
  - Neutrinos (very difficult on current sensitivity)
  - Cosmic rays (e.g. Galactic remnant; Kimura+18, ApJ, 866, 51)
  - sGRB precursor, extended/plateau emission from remnant activities
  - Fast radio bursts? (e.g. Totani, 13, PASJ, 65, 12)

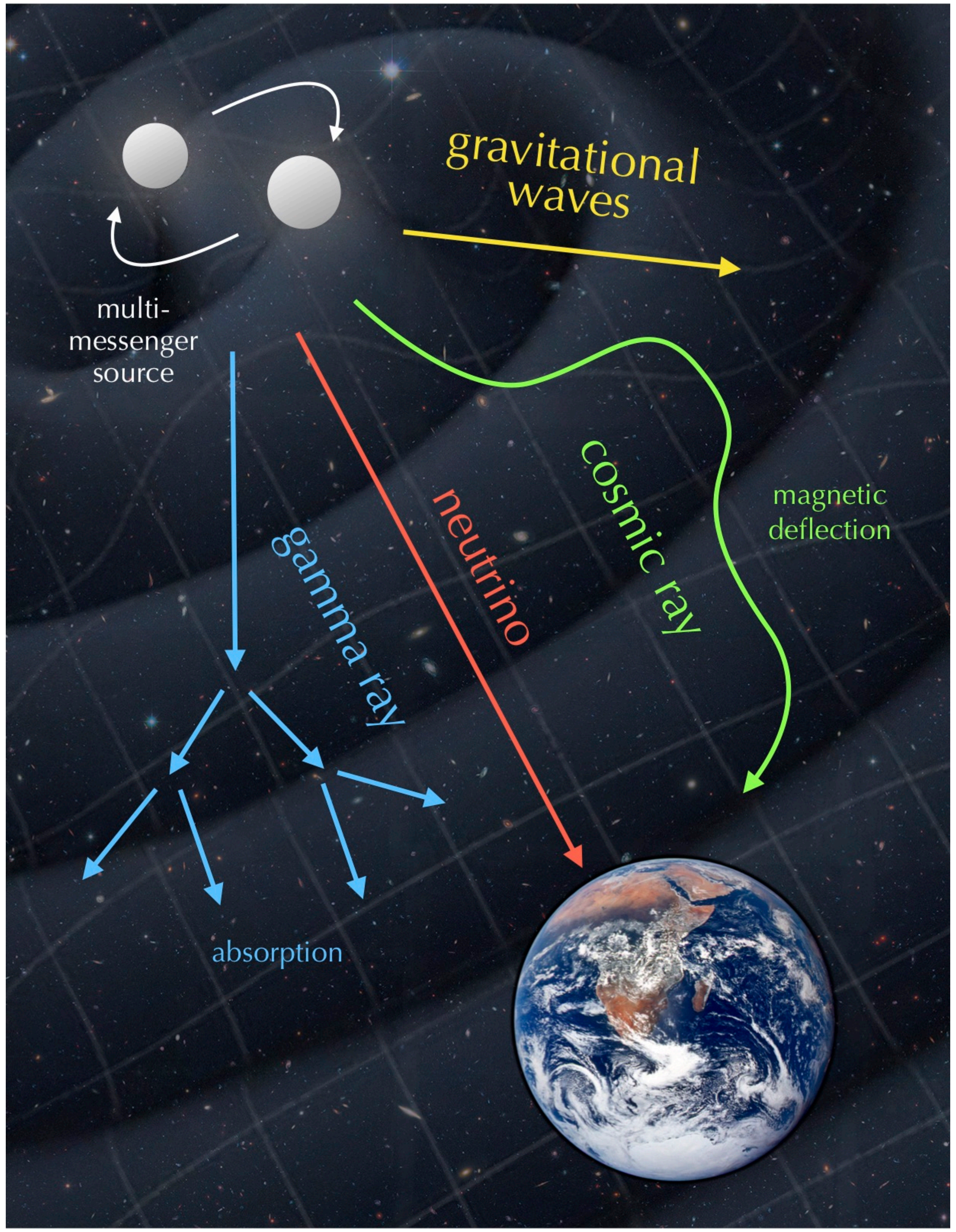


CREDIT: NIELS BOHR INSTITUTE

# Multi-messenger detection prospect of BNS merger with CTA

Very-high-energy (VHE) photon detections from 6 GRBs, including 1 sGRB*

- Challenge of particle acceleration model and GRB theory (e.g. GRB 190829A)
- Potential counterpart of GW events (GW170817 + sGRB 170817A)
- Multi-messenger prospect by future Cherenkov projects (e.g. CTA, LHAASO, SWGO)

X-ray + TeV afterglow data impose new constraint (H.E.S.S.+21, Sci, 372, 1081)

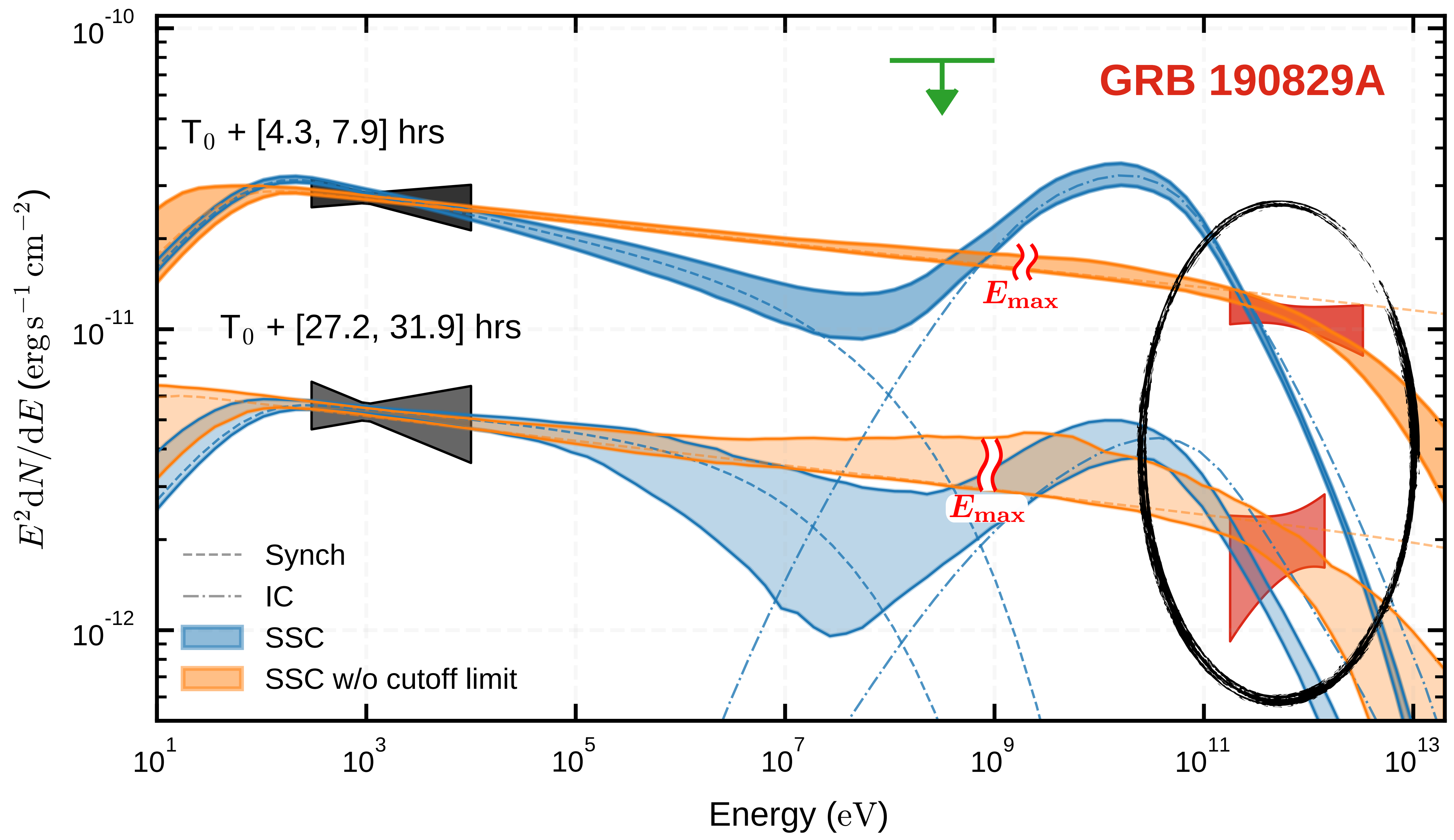


CTA can ideally scan over GW region in ~ min timescale (Bartos+19, MN, 490, 3476)

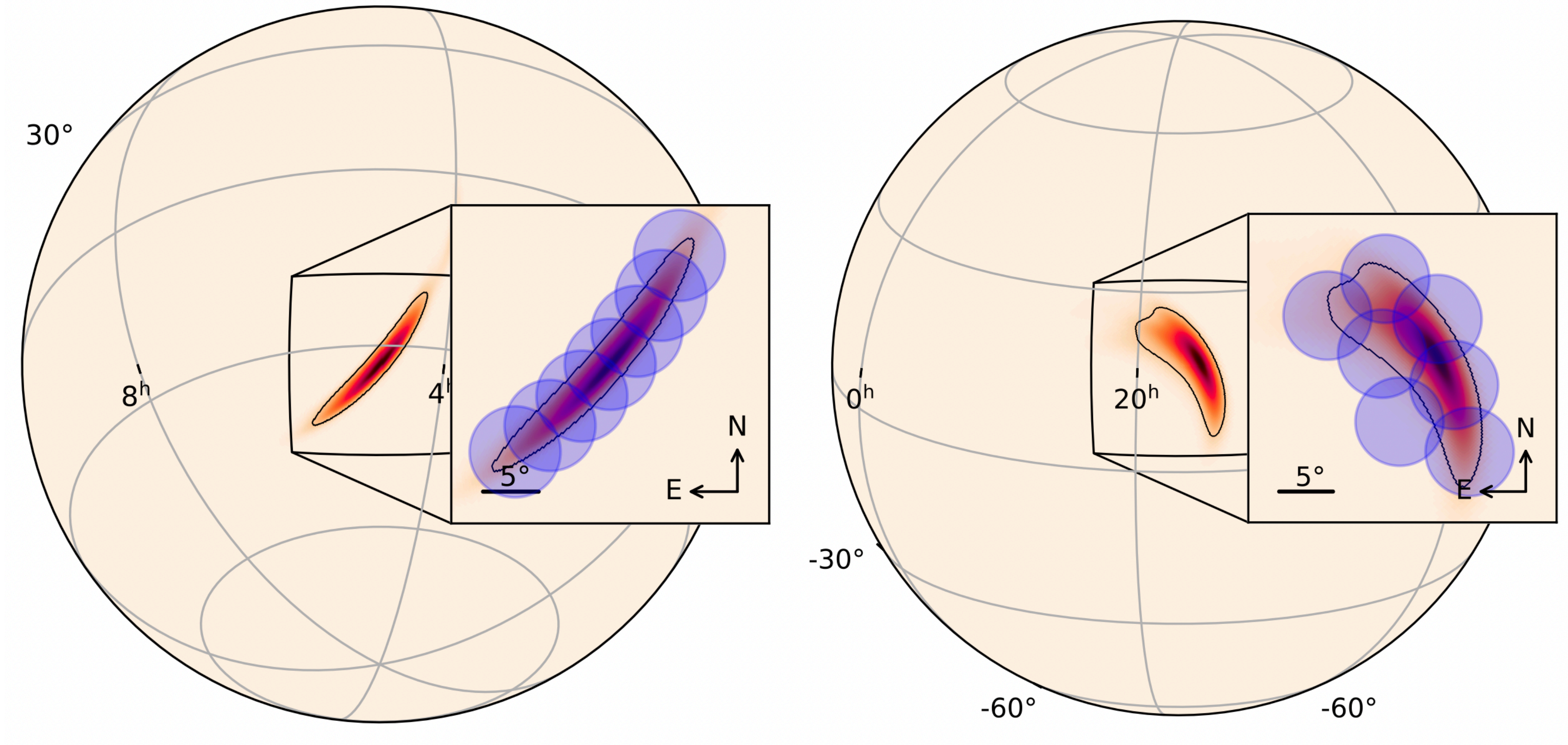


*tevcat.uchicago.edu

# A caveat in MM detectability: Malmquist bias

Say, two neutron star merge and release GWs and a GRB, then because of their common **dependency** on e.g. BNS inclination

$$\Pr(\mathrm{GW} \cap \mathrm{GRB}) \neq \Pr(\mathrm{GW}) \times \Pr(\mathrm{GRB})$$

What results from this dependency is **non-trivial** and significantly affects **joint detection rate**

$$\Pr(\mathrm{GW} \cap \mathrm{GRB}) = \Pr(\mathrm{GW}) \times \Pr(\mathrm{GRB} \mid \mathrm{GW})$$

By Bayesian conditional probability

$$\approx 3.4 \times \Pr(\mathrm{GW}) \times \Pr(\mathrm{GRB})$$

By Schutz, 2011, CQGra, 28, 125023

will be 1.26 times the search threshold. For binary systems, I also derive the universal pdf for detected values of the orbital inclination, taking into account the Malmquist bias; this implies that the number of gamma-ray bursts associated with detected binary coalescences should be 3.4 times larger than expected from just the beaming fraction of the gamma burst. Using network antenna patterns, I propose three figures of merit

This bias is frequently ignored in MM detection rate study.

# A caveat in MM detectability: Malmquist bias

$$\Pr(\mathrm{GW} \cap \mathrm{GRB}) \approx 3.4 \times \Pr(\mathrm{GW}) \times \Pr(\mathrm{GRB})$$

$$\downarrow$$

Moreover, this factor may not be the final answer yet:

- GRB was assumed always detectable on-axis and invisible otherwise, inconsistent with GRB 170817A which was detected off-axis
- No discussion for latency time between GW and GRB
- Cosmological evolution of GRB/BNS rate ignored
- Binary polarization angle was ignored (minor)

We need to carefully improve the formulation to allow general discussion.

# Population model of MM detectability

Let's simulate a large sample of population. The parameters of population (e.g. orientation, burst and observation) follow prior distributions $\mathcal{P}_X$. We quantify the detection probability as the number fraction that meets **MM detection criteria**:

$$\Pr(\text{criteria}) \equiv \int_{\text{criteria}(X)} \mathcal{P}_X \, dX$$

$$X = \{\theta, \phi, \psi, \iota; E_{\text{iso}}, n_{\text{ISM}}, \theta_{\text{jet}}, \ldots; D_L, F_{\text{sen}}, t_{\text{latency}}, t_{\text{exposure}} \ldots\}$$

A source is MM detectable, if it stays within the **minimum visibility distance** $\mathcal{D}_v$ at which all messengers of interest are visible:

$$\text{criteria}: D_L < D_v \equiv \min(D_{\text{GW}}, D_{\text{GRB}}, \ldots)$$

# Visibility distance: gravitational waves

$$D_{\rm GW}^2 \propto \Theta^2(\theta, \phi, \iota, \psi; \beta_i, \lambda_i, \chi_i)$$

$\Theta^2$ : response pattern of detector network

$\theta, \phi, \iota, \psi$ : inclination angles

$\beta_i, \lambda_i, \chi_i$ : latitude, longtitude, orientation of $i$-th detector

Explicit form are given in Schutz, 2011, CQGra, 28, 125023

Normalization is given in Abbott et al., 2018, LRR, 21, 3

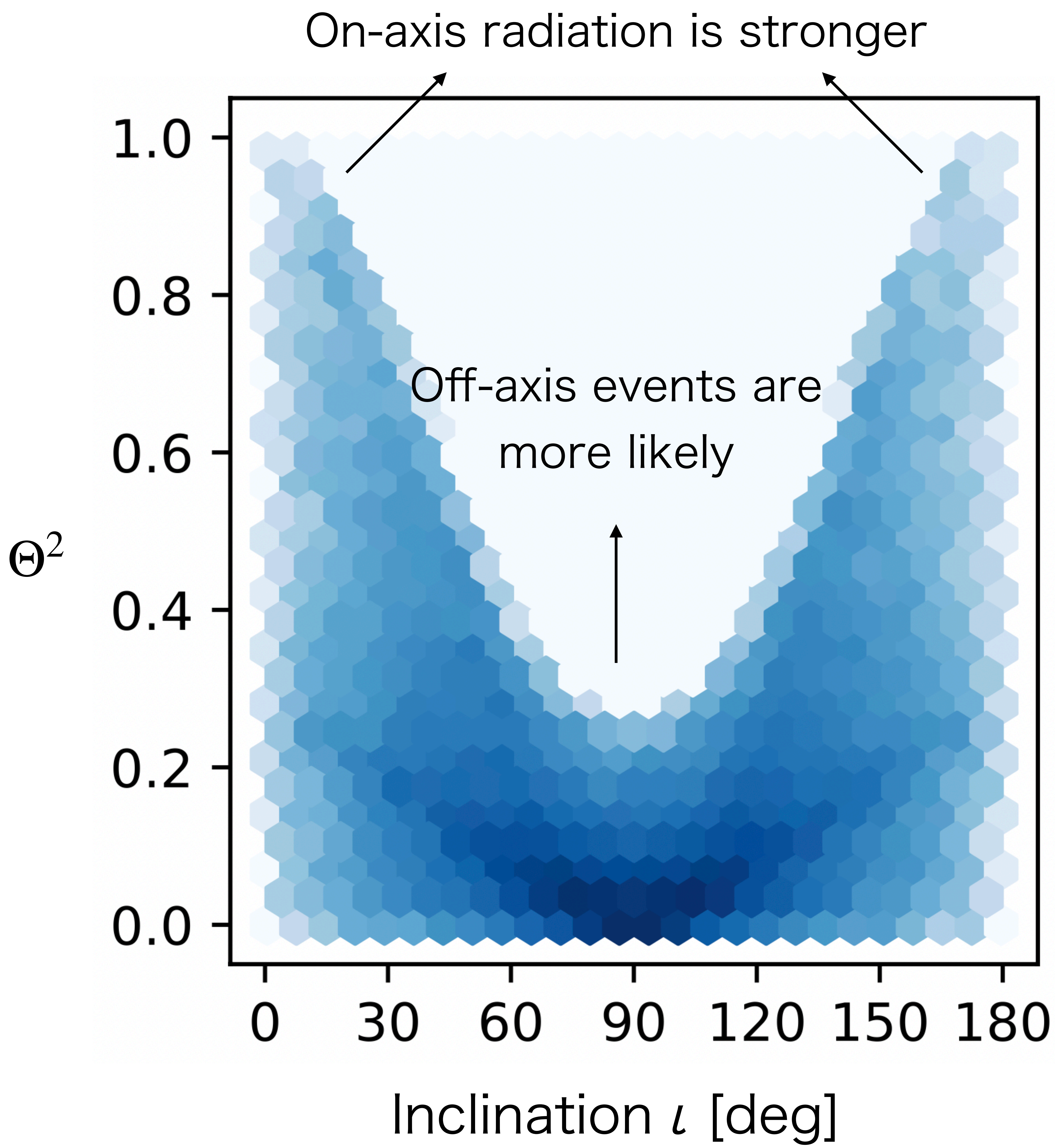

# Visibility distance: GRB afterglow (< TeV)

$$D_{\rm GRB}^2 = \frac{L}{4\pi F_{\rm sen}}$$

L: synchrotron+inverse-Compton GRB **afterglow** spectra, powered by a Gaussian-structured jet with ~ 5 deg width (consistent with GW170817 and sGRB jet break data)

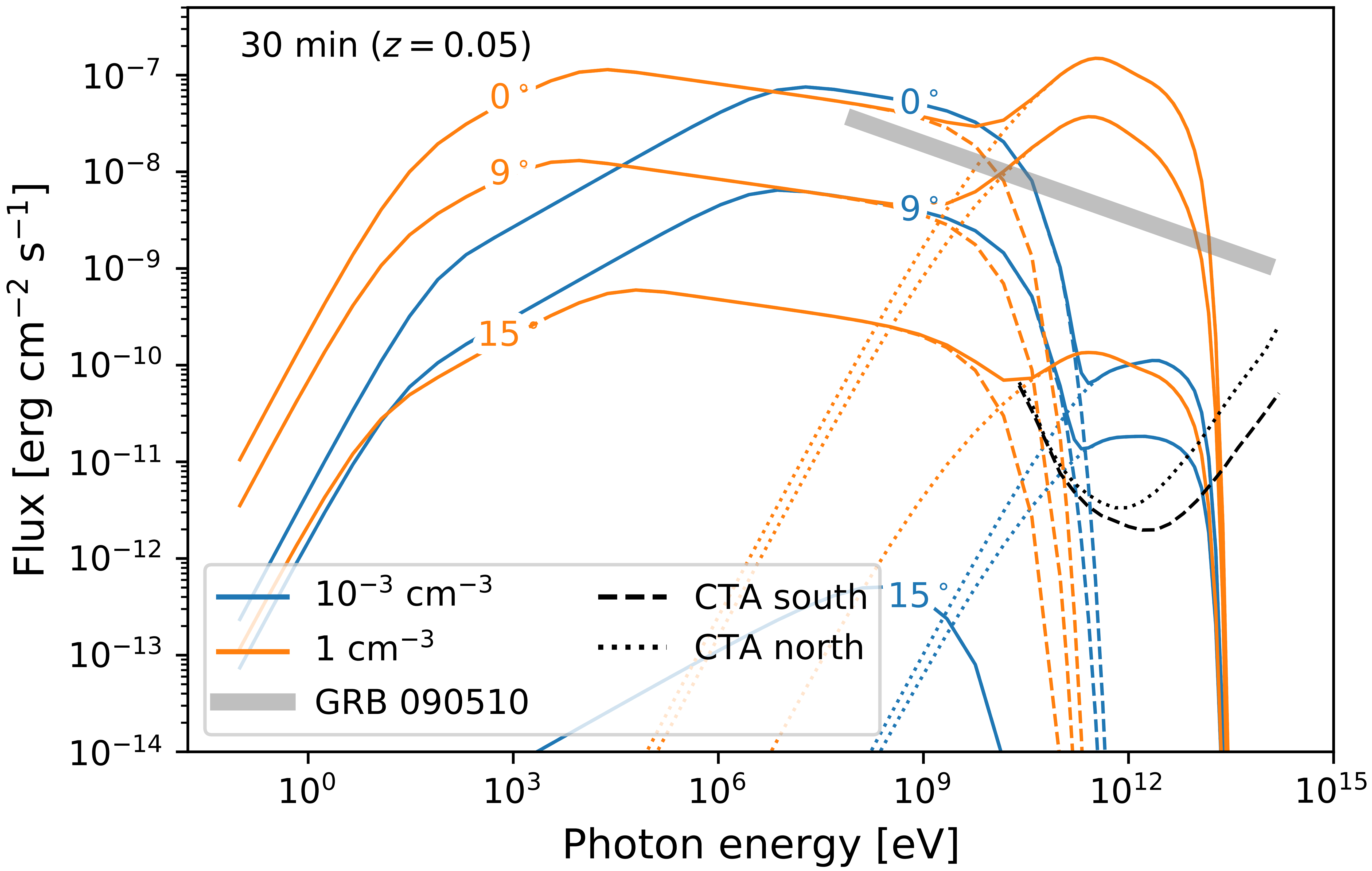


Off-axis is also detectable!

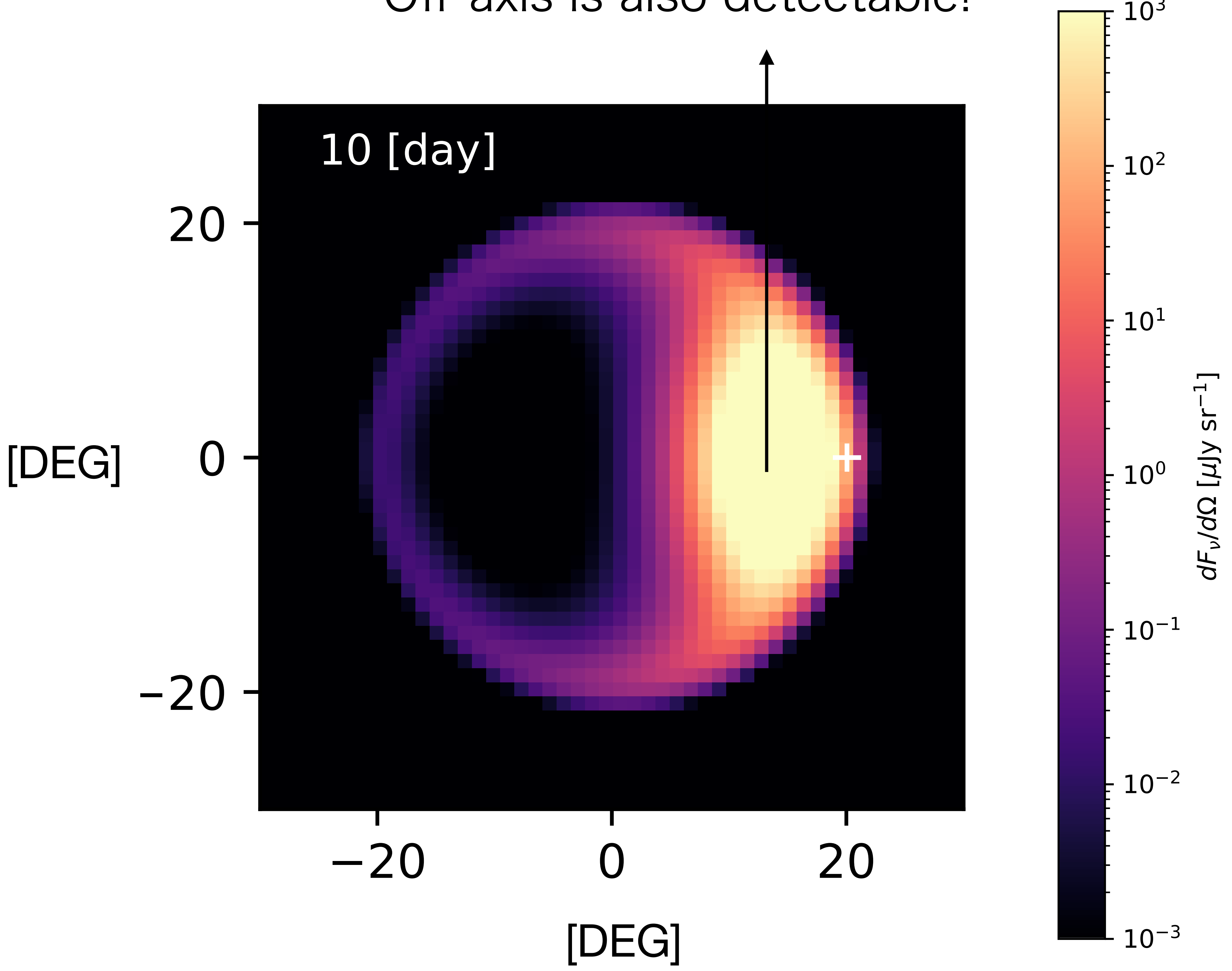

# Visibility distance: GRB TeV gamma-ray afterglow

$$D_{\rm CTA} = \frac{2}{\kappa_{\rm EBL}} W_0 \left( \frac{\kappa_{\rm EBL}}{2} \sqrt{\frac{L}{4\pi F_{\rm sen}}} \right)$$

$$L = \frac{1}{t_{\rm exp}} \int_{t_{\rm lat}}^{t_{\rm lat}+t_{\rm exp}} L_{\rm jet}\, dt \qquad F_{\rm sen} = F_{\rm CTA}(t_{\rm exp})$$

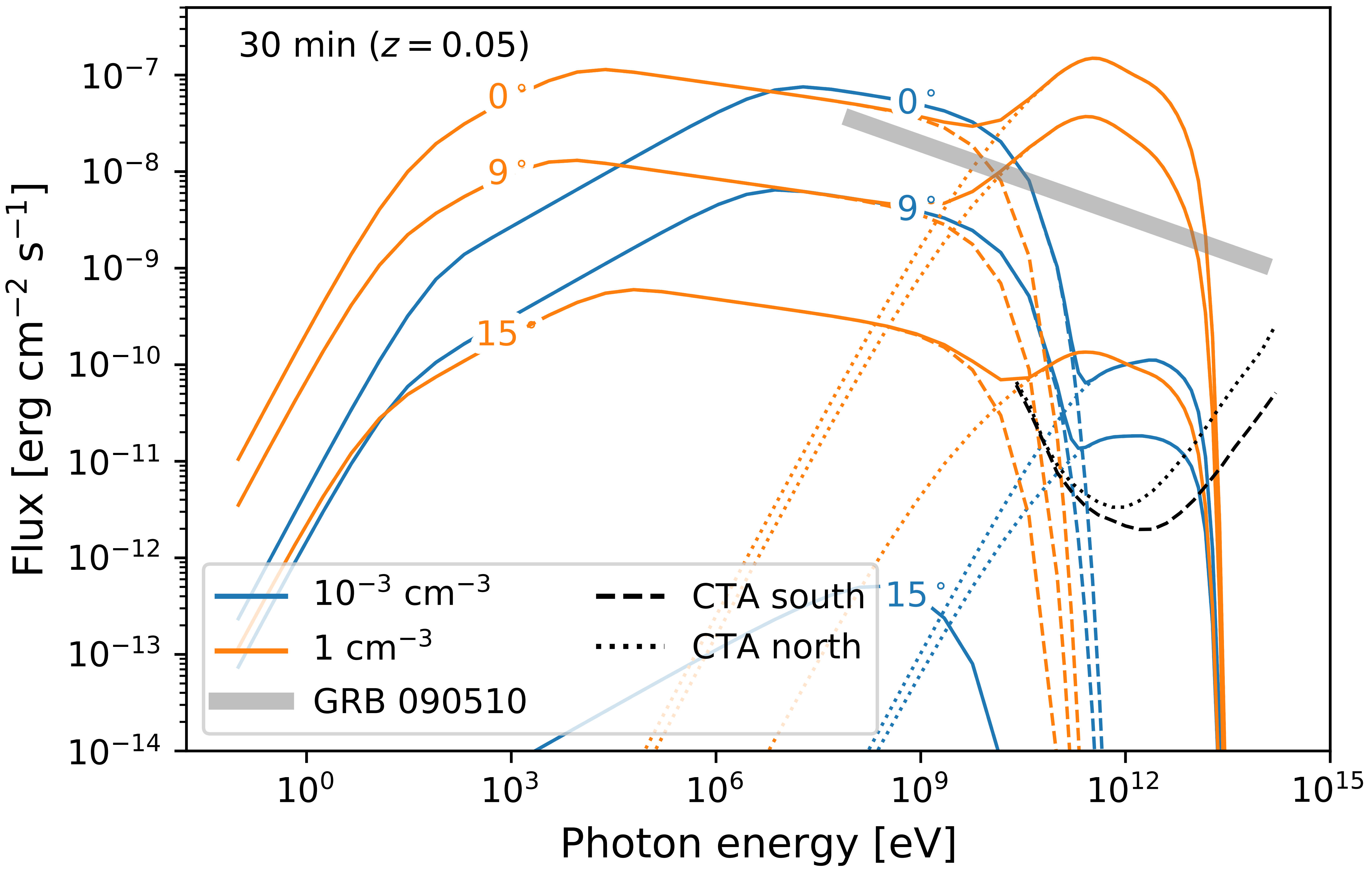


$\kappa_{\rm EBL}$ (Extragalactic Background Light)

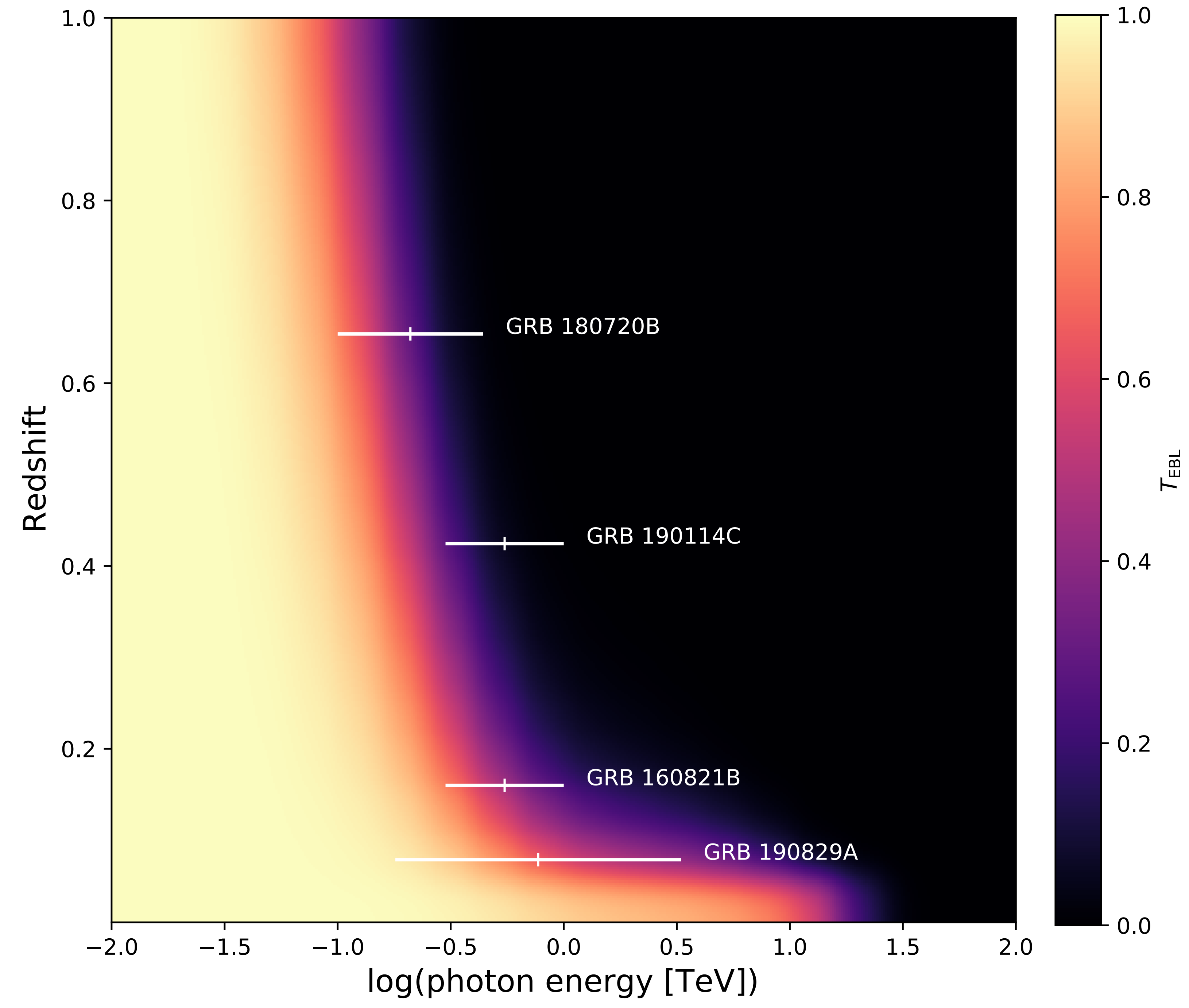

# Population model: MM detection rate

Marginalizing out all parameters, we obtain the **MM detection rate**:

$$N = \int \Pr(D_L) \frac{R_{\rm BNS}(z)}{1+z} 4\pi D_L^2 \, dD_L \approx \frac{4\pi}{3} \langle D_v^3 \rangle_X \, R_{\rm BNS}(0)$$

(Exact) (Cosmic evolution ignored)

where $\langle D_v^3 \rangle_X = \int \min(D_{\rm GW}, D_{\rm EM}, \ldots)^3 \, \mathscr{P}_X \, dX$

But we don't actually do the integral. Take the **Monte-Carlo** shortcut:

$$X \sim \mathscr{P}_X \implies \begin{aligned} \Pr(D_L) &\approx \frac{1}{k} \sum_{i=1}^{k} H(D_{\rm GW,i}^2 - D_L^2) H(D_{\rm GRB,i}^2 - D_L^2) \\ \langle D_v^3 \rangle_X &\approx \frac{1}{k} \sum_{i=1}^{k} \min(D_{{\rm GW},i}, D_{{\rm GRB},i}, \ldots)^3 \end{aligned}$$

# Population model: MM Malmquist bias

Marginalizing out all parameters but leaving one of interest (x), we obtain the **Malmquist bias** for x:

$$\mathscr{M}_x \equiv \frac{\left\langle D_v^3 \right\rangle_{X/x}}{\left\langle D_v^3 \right\rangle_X} = \frac{\mathscr{P}_x |_{\rm obs}}{\mathscr{P}_x |_{\rm prior}}$$

Similarly, it can be evaluated via Monte-Carlo.

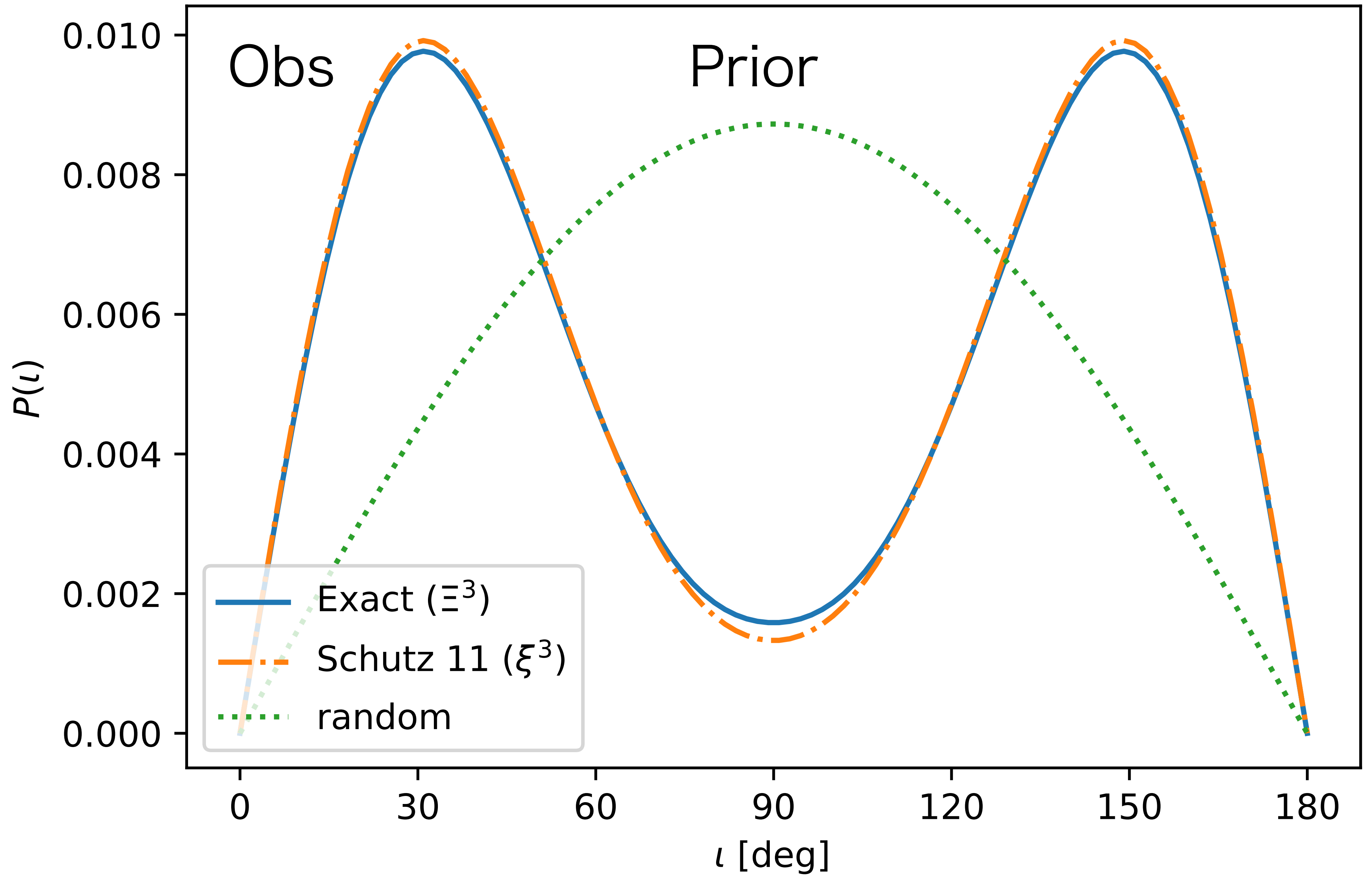


When x = $\iota$ (BNS inclination angle) and $D_{GW} \ll D_{GRB}$, $\mathscr{M}_\iota |_{\iota=0} = 3.4$

$$\mathscr{P}_\iota \Big|_{\rm obs} \propto \left\langle \Theta^3 \right\rangle_{\{\theta,\phi,\psi\}} \approx \left\langle \Theta^2 \right\rangle^{3/2}_{\{\theta,\phi,\psi\}} = 0.076\,(\cos^4\iota + 6\cos^2\iota + 1)^{3/2} \sin\iota$$

(Seto, 2014, MNRAS, 446, 2887) (Schutz, 2011, CQGra, 28, 125023)

# Application to BNS detectability with LIGO+CTA

## CONFIGURATION

**Population simulation**: ~ 10^5 random sampling from prior distributions based on assumptions or short GRB observations

**GW**: response pattern of single detector normalized to LIGO O5 sensitivity

**GRB**: synchrotron self-Compton afterglow by a Gaussian-structured jet + CTA south sensitivity (100s & 30m exposure, 5m latency from GW onset, 20deg zenith)

Table 4.1: Summary of population model parameters

| Physical quantity | Parameter $X$ | Distribution $\mathcal{P}_X$ |
|---|---|---|
| Isotropic energy (jet) | $\log(E_0\|_{\rm jet}\,[\rm erg])$ | $\mathcal{G}(\mu = 51.2, \sigma = 0.83)$ |
| Initial Lorentz factor (jet) | $\Gamma_0\|_{\rm jet}$ | 1000 |
| Half-opening angle (jet) | $\theta_j\,[\rm deg]$ | $\mathcal{G}(\mu = 5.8, \sigma = 1.2)$ |
| Isotropic energy (ejecta) | $\log(E_0\|_{\rm ej}\,[\rm erg])$ | 51 |
| Bulk velocity (ejecta) | $\beta_0\|_{\rm ej}$ | 0.3 |
| Stratification (ejecta) | $k$ | $\infty$ |
| CBM density | $\log(n_0\,[\rm cm^{-3}])$ | $\mathcal{G}(\mu = -1.57, \sigma = 1.63)$ |
| CBM profile index | $s$ | 0 |
| Magnetic field energy | $\epsilon_B$ | 0.01 |
| Non-thermal electron energy | $\epsilon_e$ | 0.1 |
| Electron spectrum index | $p$ | $\mathcal{G}(\mu = 2.39, \sigma = 0.23)$ |
| Electron injection efficiency | $f$ | 1 |
| Zenith | $\cos\theta$ | $\mathcal{U}(-1, 1)$ |
| Azimuth | $\phi$ | $\mathcal{U}(0, 2\pi)$ |
| BNS inclination | $\cos\iota$ | $\mathcal{U}(-1, 1)$ |
| BNS polarization | $\psi$ | $\mathcal{U}(0, 2\pi)$ |

$\mathcal{G}$ stands for Gaussian distribution and $\mathcal{U}$ stands for uniform random distribution.

# Sampling distribution based on short GRB observation

$\mathscr{P}_{\mathrm{sGRB}}$

(Fong+15, ApJ, 815, 102)

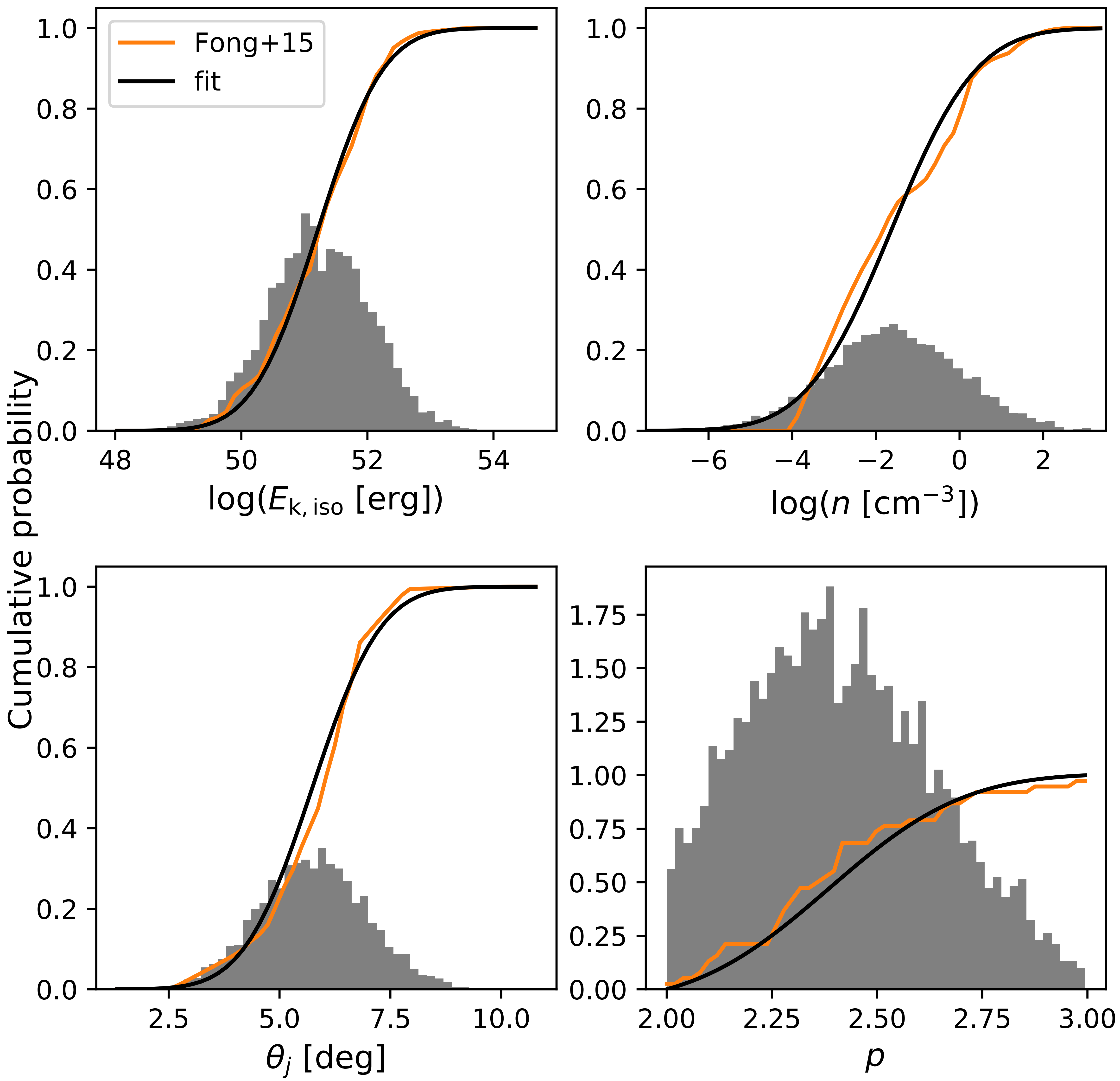

# BNS detectability with LIGO+CTA

| | LIGO | CTA | | LIGO-CTA | |
|---|---|---|---|---|---|
| **Config** | O5 | exp100s | exp30m | exp100s | exp30m |
| **max($D_v$) [Mpc]** | 747 | 4905 | 5867 | 701 | 710 |
| **$\langle D_v^3\rangle^{1/3}$ [Mpc]** | 330 | 246 | 300 | 76 | 84 |
| **$\langle D_v^3\rangle/\langle D_{GW}^3\rangle$** | 100% | 41.4% | 75% | 1.2% | 1.6% |
| **Rate [yr^-1]*** | 48.2 | 3.0 | 5.43 | 0.09 | 0.12** |

Max distance CTA >> LIGO

Detection rate CTA < LIGO

*BNS merger rate = 320 [Gpc^-3 yr^-1] is assumed (Abbott+21, ApJ, 913, L7) CTA duty cycle = 15%. Latency from GW = 5 min.

**0.03 [yr^-1] rescaled from Patricelli+18, JCAP, 05, 056.

# GW+VHE joint detectability with LIGO+CTA

**Malmquist Bias** $\mathscr{M}_x \equiv \frac{\left\langle D_v^3 \right\rangle_{X/x}}{\left\langle D_v^3 \right\rangle_X} = \frac{\mathscr{P}_x|_{\mathrm{obs}}}{\mathscr{P}_x|_{\mathrm{pri}}}$

- Trivially, detection is easier with smaller $D_L$, smaller $\iota$ and larger $E_{\mathrm{k,iso}}$.
- **Intermediate $n$ is favored**. Likely, while small $n$ lowers the afterglow flux, large $n$ decelerates the shock too much before CTA can follow up.
- **Constraint from MM observation**: since we know the priors for $D_L$ and $\iota$, their observed distributions $\mathscr{P}|_{\mathrm{obs}}$ can in principle impose constraint on the emission model → working on it.

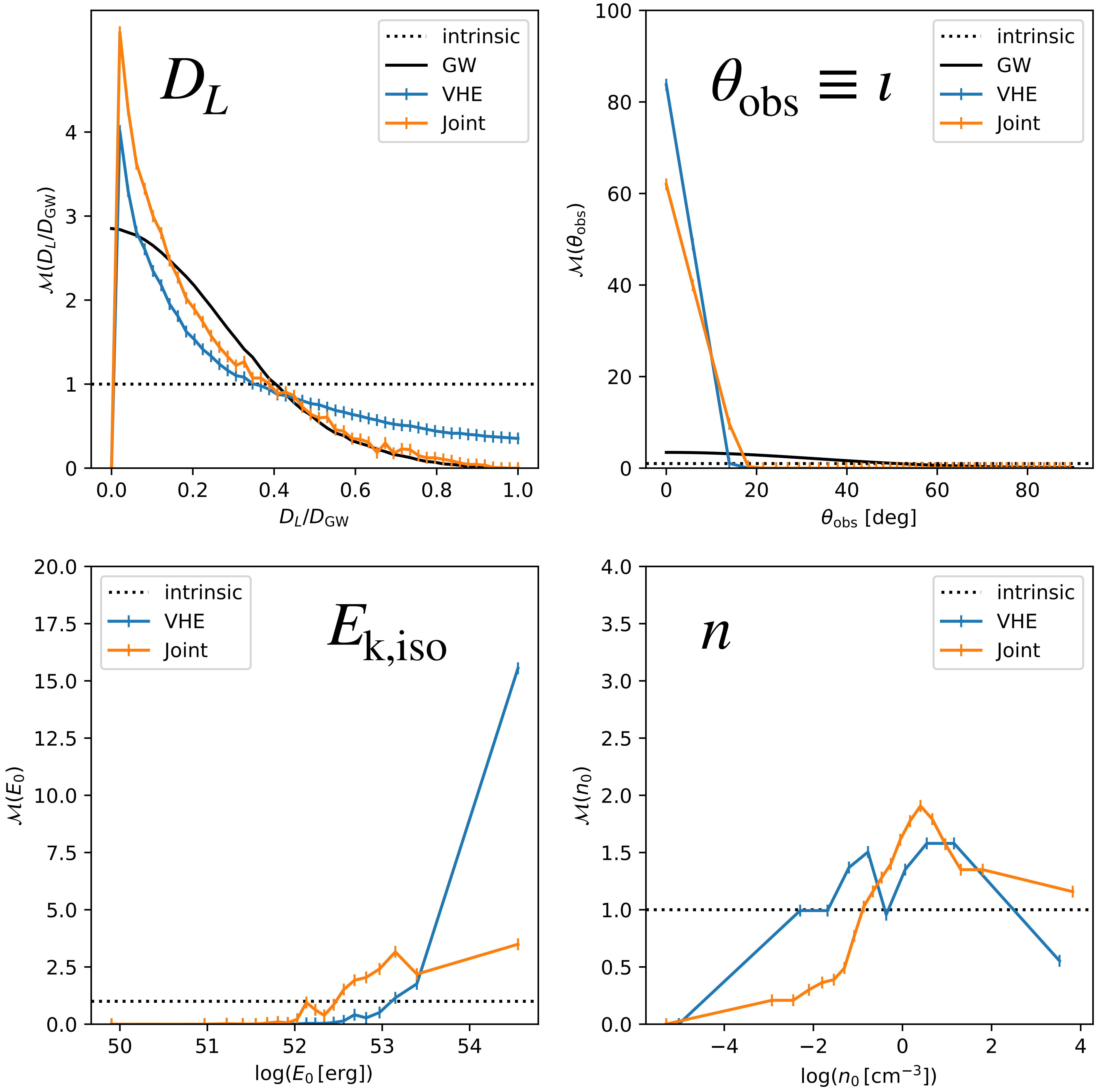

# Optimized observation with LIGO+CTA

$$\frac{\Pr(\mathrm{GW} \cap \mathrm{GRB})}{\Pr(\mathrm{GW}) \times \Pr(\mathrm{GRB})}$$

$t_{\mathrm{delay}}$: delay time between LIGO and CTA. The smaller the better.

$t_{\mathrm{exp}}$: CTA exposure duration. Optimized between 1 and 30 min.

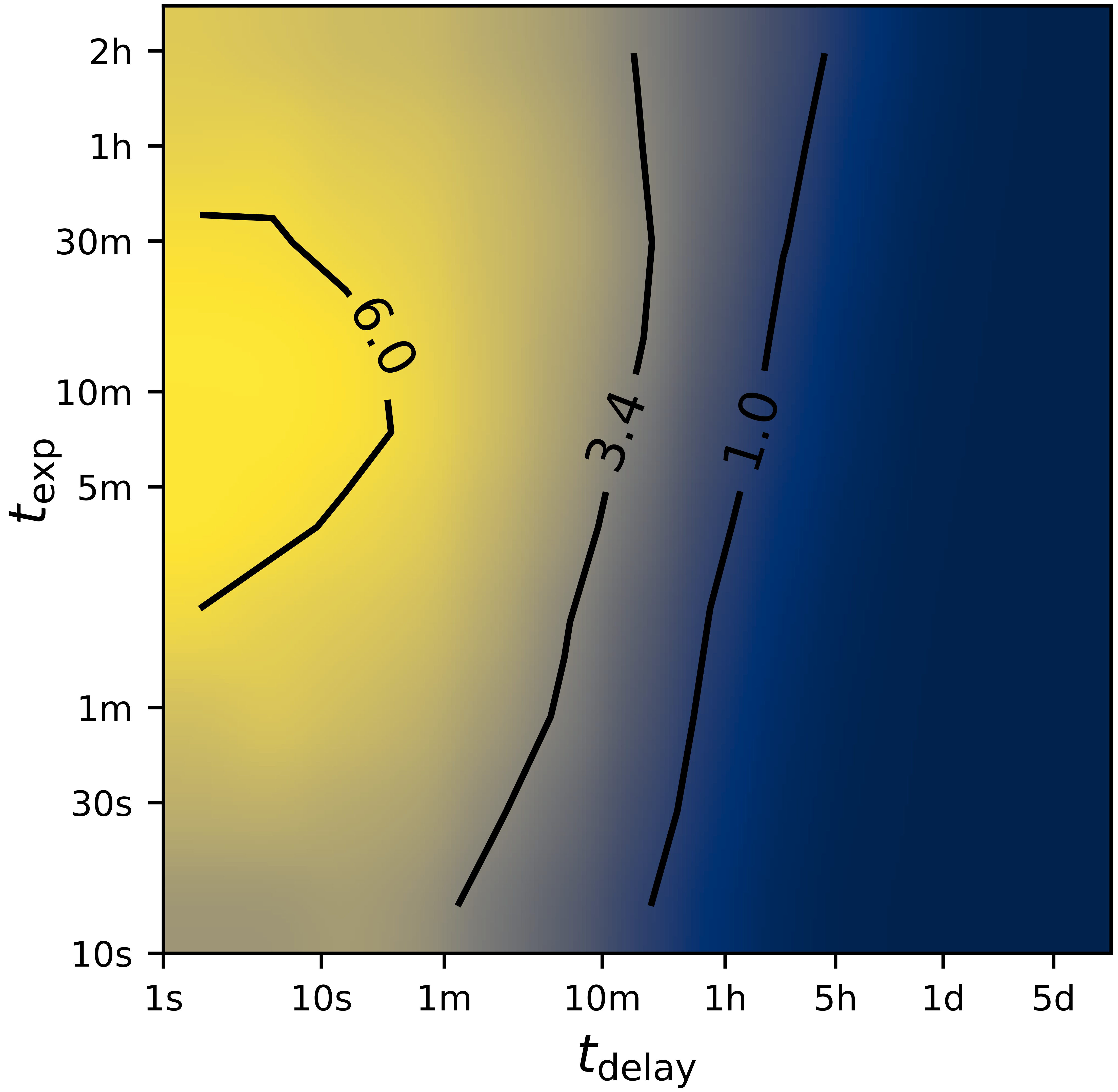

# Bonus: constraint on FRB progenitor model

We examined if Fast Radio Burst are associated with BNS afterglow, whether or not the observational limit would be violated:

$$\mathrm{Pr}(F_{\mathrm{afterglow}} < F_{\mathrm{obs\,lim}} \,|\, \mathrm{FRB} + \mathrm{afterglow}) \ll 1\,?$$

Number of observations expected for a joint FRB+afterglow detection

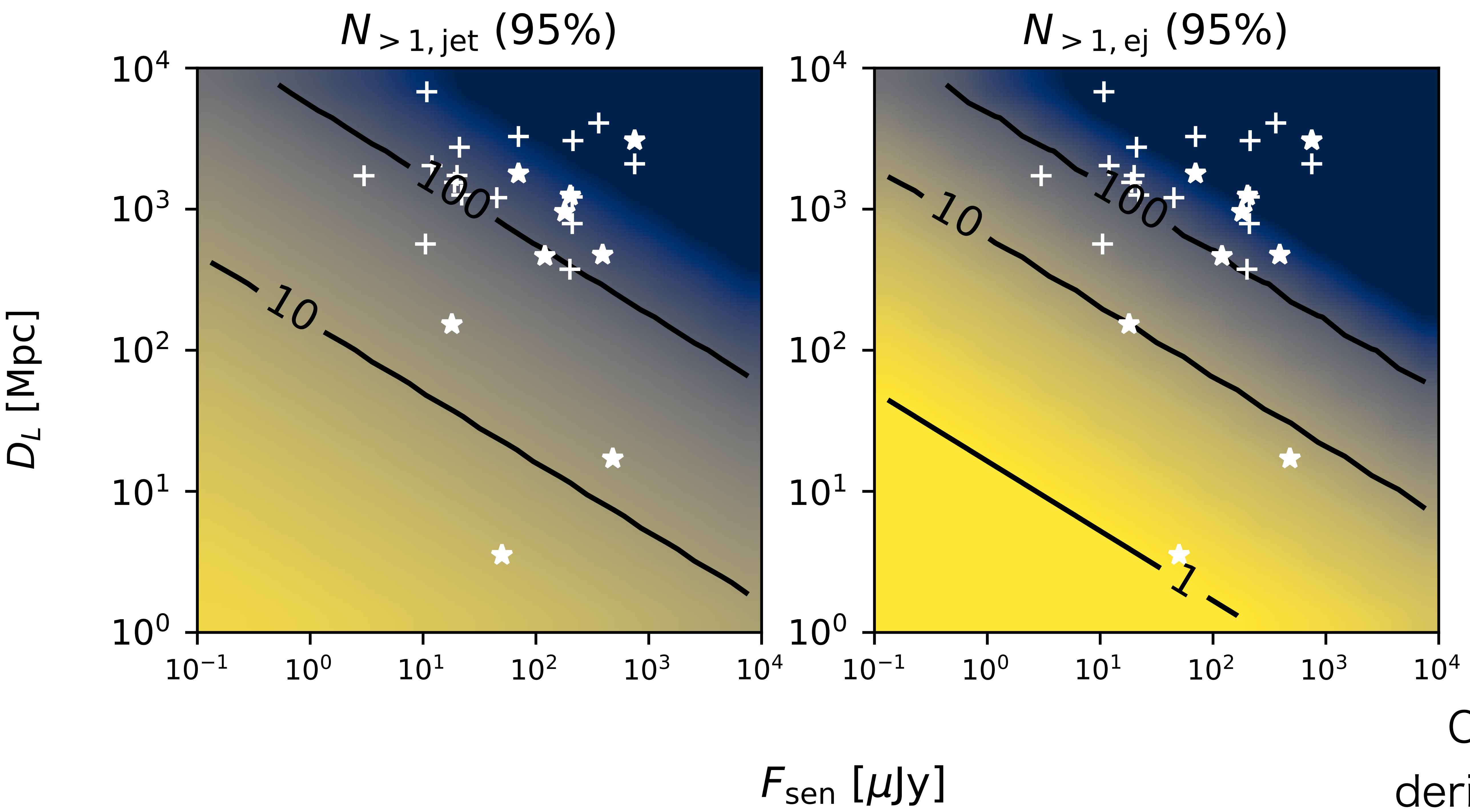


Comparison with observational upper limits on FRBs

| FRB | $z$[a] | DM [pc cm$^{-3}$] | $F_{\mathrm{sen}}$ [μJy][b] | $\nu_{\mathrm{sen}}$ [GHz][b] | $P_{\mathrm{jet}}$ ($P_{\mathrm{ej}}$)[c] | Reference |
|---|---|---|---|---|---|---|
| 121102* | 0.19 | 558.0 | 180.0 | 1.6 | 1% (0.6%) | Chatterjee et al. (2017) |
| 180301* | 0.33 | 536.0 | 70.0 | 1.5 | 1% (0.5%) | Bhandari et al. (2021) |
| 180814* | <0.11 | 189.0 | 390.0 | 3.0 | 2% (1%) | CHIME/FRB Collaboration et al. (2019a) |
| 180916B* | 0.0337 | 349.0 | 18.0 | 1.6 | 15% (26%) | Marcote et al. (2020) |
| 181030A* | 0.00385 | 103.5 | 480.0 | 3.0 | 18% (40%) | Bhandari et al. (2021) |
| 190520* | 0.241 | 1202.0 | 202.0 | 3.0 | 0.9% (0.4%) | Niu et al. (2021) |
| 190711* | 0.522 | 587.4 | 750.0 | 0.9 | 0.1% (0%) | Macquart et al. (2020) |
| 200120E* | 0.0008 | 87.0 | 50.0 | 1.4 | 48% (72%) | Kirsten et al. (2021a) |
| 201124A* | 0.098 | 420.0 | 120.0 | 1.4 | 4% (4%) | Ravi et al. (2021) |
| 131104 | <0.55 | 779.0 | 45.0 | 5.5 | 0.6% (0.2%) | Shannon & Ravi (2017) |
| 171020 | <0.08 | 114.0 | 120.0 | 2.1 | 4% (3%) | Mahony et al. (2018) |
| 180309 | <0.32 | 263.0 | 17.1 | 3.0 | 3% (6%) | Aggarwal et al. (2021) |
| 180924 | 0.3214 | 361.4 | 20.0 | 6.5 | 3% (2%) | Bannister et al. (2019) |
| 181112 | 0.4755 | 589.3 | 21.0 | 6.5 | 2% (0.8%) | Prochaska et al. (2019) |
| 190102 | 0.2913 | 364.5 | 19.0 | 6.5 | 3% (2%) | Bhandari et al. (2020a) |
| 190523 | 0.66 | 760.8 | 360.0 | 3.0 | 0.1% (0%) | Ravi et al. (2019) |
| 190608 | 0.11778 | 339.5 | 10.5 | 6.5 | 8% (11%) | Bhandari et al. (2020a) |
| 190611 | 0.378 | 321.4 | 750.0 | 0.9 | 0.2% (0%) | Heintz et al. (2020) |
| 190614D | <1.0 | 959.2 | 10.8 | 1.4 | 0.8% (0.4%) | Law et al. (2020) |
| 190714 | 0.2365 | 504.1 | 210.0 | 3.0 | 0.9% (0.4%) | Heintz et al. (2020) |
| 191001 | 0.234 | 506.0 | 45.0 | 5.5 | 2% (2%) | Bhandari et al. (2020b) |
| 191108 | <0.52 | 588.1 | 213.0 | 1.4 | 0.3% (0%) | Connor et al. (2020b) |
| 191228 | 0.243 | 297.5 | 22.0 | 6.5 | 3% (3%) | Bhandari et al. (2021) |
| 200430 | 0.16 | 380.1 | 210.0 | 3.0 | 2% (0.9%) | Heintz et al. (2020) |
| 200906 | 0.3688 | 577.8 | 12.0 | 6.0 | 3% (2%) | Bhandari et al. (2021) |

* Repeating FRB sources

Conclusion: we still need ~100 or 10x current sample to derive meaningful constraint (Lin, Totani, 20, MN, 498, 2384)

# Conclusion

- A formulation for multi-messenger detectability and Malmquist bias is presented
- Following results have been obtained by now on BNS detectability:
  - Maximum reach CTA >> LIGO, but detection rate CTA << LIGO
  - LIGO-CTA joint detection rate ~ 0.1 per year
  - Taking into account Malmquist bias boosts joint detection rate by ~ x3
- To-do list in the future:
  - Detectability with LVK-CTA; with EAS arrays such as LHAASO, SWGO (lower sensitivity but greater FoV and ~100% duty cycle)
  - Add cosmic ray, neutrino into discussion $D_\nu(X) = \min\left(D_{\rm GW}, D_{\rm EM}, D_{\rm CR}, D_\nu, \ldots\right)$